

# PARALLEL TRANSMISSION DESIGN OF MULTI-PULSE SEQUENCES USING SPATIALLY RESOLVED EXTENDED PHASE GRAPHS (SREPG)

S. J. Malik<sup>1</sup>, H. Homann<sup>2</sup>, P. Börner<sup>3</sup>, and J. V. Hajnal<sup>1</sup>

<sup>1</sup>Robert Steiner MRI Unit, Imaging Sciences Department, MRC Clinical Sciences Centre, Hammersmith Hospital, Imperial College London, London, London, United Kingdom, <sup>2</sup>Institute of Biomedical Engineering, Karlsruhe Institute of Technology, Karlsruhe, Germany, <sup>3</sup>Philips Research, Hamburg, Germany

**Introduction** The extended phase graph (EPG) algorithm provides an elegant framework for calculating signal intensities ( $S(t)$ ) for experiments involving multiple Radio Frequency (RF) pulses [1]; an important application is for pulse trains with temporally varying flip angles  $\alpha(t)$  i.e.  $S(t) = f(\alpha(t))$ , where  $t$  is time and  $f$  represents application of the EPG algorithm. If the RF field ( $B_1$ ) is spatially varying, such as is generally the case at high field strength (3T+), a single EPG calculation is no longer sufficient to predict signals throughout the object. In many circumstances this variable response is a problem, however the active control of the  $B_1$  field afforded by parallel transmission (PTx) makes this an opportunity. In this regime it is natural to include a spatial dimension into the EPG, resulting in a Spatially Resolved EPG (SREPG). We have explored designing with SREPG, focusing initially on the fast spin echo (FSE) sequence, since this family has been studied in detail using conventional EPG [2]. For SREPG, the signals and flip angles become explicitly spatially dependent,  $S(r,t) = f(\alpha(r,t))$ , and in the case of PTx,  $\alpha(r,t) = \sum_c \sigma_c(r) \alpha_c(t)$ , where  $\sigma_c(r)$  is the transmit sensitivity of channel  $c$  and  $\alpha_c(t)$  is the drive (complex amplitude) applied to it. A limited case is when the coil drives retain a fixed relationship and are simply scaled together over time. We term this "static" RF shimming. A more general solution allows for the application of different sets of drives for each RF pulse in order to manipulate the signal behaviour differently for each location in space; we term this "dynamic" RF shimming.

**Methods** For an FSE pulse sequence with  $N_{\text{echo}}$  refocusing pulses the amplitude and phase of  $N_{\text{echo}}+1$  pulses (including the excitation pulse) can be independently adjusted on each of the  $N_c$  channels. In this work we have explored the flexibility of this framework by optimizing these variables with respect to the following cost function:

$$\min \left\{ \left\| T(r,n) - \left[ f \left( \sum_c \sigma_c(r) \alpha_c(n) \right) \right] \right\|_{W(r,n)}^2 + \lambda \left\| \alpha_c(n) \right\|^2 \right\} \quad \text{using the SREPG approach to compute the signals in each iteration.}$$

Here  $W$  corresponds to a weighting function and  $T$  is the target signal magnitude, both of which are functions of space and echo number,  $n$ . Parameter  $\lambda$  is used to control total RF power. Optimisation was performed using the pattern search algorithm, implemented as part of the Matlab (The Mathworks) Direct Search toolbox. In order to reduce the computational load a limited set of voxels was considered in each optimisation. Experiments were performed using a Philips 3T Achieva MRI system with an 8-channel parallel transmission body coil [3] using two separate phantoms; (i) a 16cm diameter spherical flask and (ii) a 40cm diameter cylinder both containing a solution of water and  $\text{CuSO}_4$ . All experiments used multi-shot FSE with 16 echoes per shot.  $B_1$  maps were acquired using the modified AFI sequence [4] with slice profile correction [5].

**Results** The small phantom was imaged using a static pseudo steady-state (SPSS) echo train computed to give a constant signal of  $0.7M_0$  using Hennig's 1-ahead algorithm [6]. This phantom induces strong  $B_1$  variation when the transmit array is in quadrature configuration. Optimised dynamic RF shims were computed by starting with this solution but with the target of producing spatially uniform signal for all echoes. Fig 1 shows the

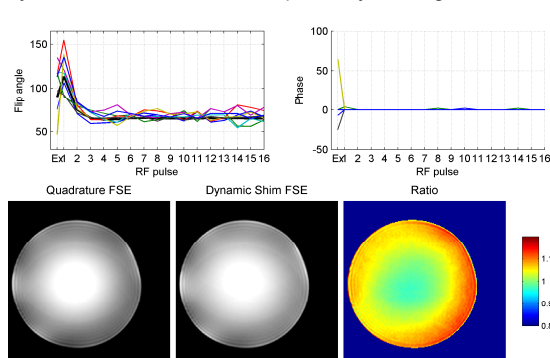


Figure 1

but produces significantly lower error; the same level of error can only be achieved with static shimming by using over 4 times more RF power than quadrature mode.

We may also choose to weight the cost function in space or as a function of echo number (using the parameter  $W$ ). This may be used, for example, to produce uniform contrast only at the echoes encoding the centre of k-space or to produce constant signal across all echoes for a limited spatial region, constraining the point-spread function (PSF). Figure 3 shows the result of an example in the larger phantom; in this case the aim was to reduce RF power while constraining the PSF only in the upper right hand part of the image, allowing resolution to be lower elsewhere. The dynamic shim solution used 44% less RF power than the standard FSE with some resolution loss outside the optimised region (e.g. red arrow in Figure 3).

**Discussion & Conclusions** We have demonstrated that optimization using SREPG can produce FSE sequences with tailored responses. Homogeneity improvement can be achieved using less RF power than static shimming since the coherent action of multiple (spatially non-uniform) pulses can provide uniform signal [8] where and when required without requiring a single uniform (and often high SAR) shim setting. Reduction of RF power and hence SAR can be achieved by modulating the signal profile through time; this is well-known, for example using TRAPS, and in some cases a trade-off is image blurring (broadening of PSF). Dynamic shimming allows this to also be a function of space which may be of interest when imaging a small structure within a large object; foetal imaging is one example. In this work we have considered only RF power; SAR is dependent on the electric field which will be different for each of the dynamic shim configurations [9]. Such pulse-to-pulse variation in the electric field may vary the locations of SAR hotspots mitigating time averaged local heating effects [10]. This could be explicitly included in the optimisation by adding an E-field model. Currently computation times range from a few minutes to hours; a more efficient approach will be the subject of future work.

**References** [1] Hennig J, JMR 1988 78:397-407 [2] Hennig J et al, MRM 2003 49:527-535 [3] Vernickel P et al, MRM 2007 58:381-389 [4] Nehrke K, MRM 2009 61:84-92 [5] Malik SJ et al, MRM 2011 In Press [6] Hennig J et al, MRM 2004 51:68-80 [7] Kassakian P, PhD UCB 2006 [8] Xu and King, Proc ISMRM 2009:174 [9] Homann H et al, Proc ISMRM 2010:104 and MRM, In Press [10] Graesslin I, et al, Proc ISMRM 2009:176

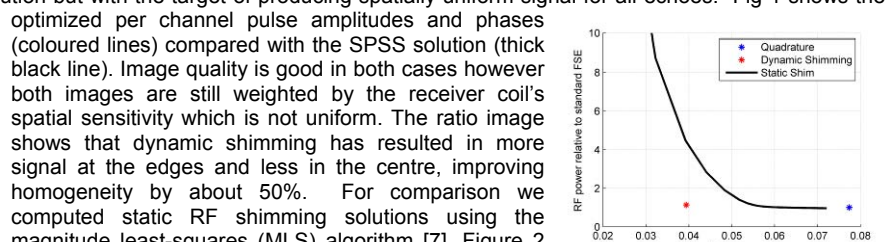


Figure 2

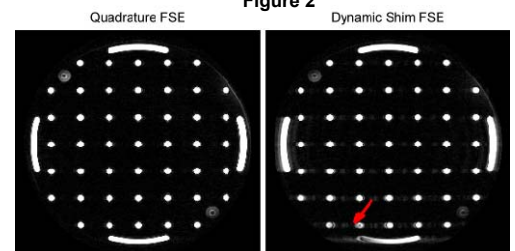


Figure 3